the FEBS Journal

Intermediate instability at high temperature leads to low pathway efficiency for an *in vitro* reconstituted system of gluconeogenesis in *Sulfolobus solfataricus*

Theresa Kouril[1], Dominik Esser[1], Julia Kort[1], Hans V. Westerhoff[2,3,4], Bettina Siebers[1] and Jacky L. Snoep[2,3,5]

1 Molecular Enzyme Technology and Biochemistry (MEB), Biofilm Centre, Faculty of Chemistry, University of Duisburg-Essen, Germany
2 Molecular Cell Physiology, Vrije Universiteit, Amsterdam, The Netherlands
3 Manchester Centre for Integrative Systems Biology, Manchester Institute for Biotechnology, University of Manchester, UK
4 Synthetic Systems Biology, University of Amsterdam, Swammerdam Institute for Life Sciences, University of Amsterdam, The Netherlands
5 Department of Biochemistry, Stellenbosch University, Matieland, South Africa

Keywords
carbon loss; mathematical model; thermal instability; thermophile

Correspondence
J. L. Snoep, Department of Biochemistry, Stellenbosch University, Private Bag X1, Matieland 7602, South Africa
Fax: +272 1808 5863
Tel: +272 1808 5844
E-mail: jls@sun.ac.za

(Received 28 March 2013, revised 4 July 2013, accepted 11 July 2013)

doi:10.1111/febs.12438

Four enzymes of the gluconeogenic pathway in *Sulfolobus solfataricus* were purified and kinetically characterized. The enzymes were reconstituted *in vitro* to quantify the contribution of temperature instability of the pathway intermediates to carbon loss from the system. The reconstituted system, consisting of phosphoglycerate kinase, glyceraldehyde 3-phosphate dehydrogenase, triose phosphate isomerase and the fructose 1,6-bisphosphate aldolase/phosphatase, maintained a constant consumption rate of 3-phosphoglycerate and production of fructose 6-phosphate over a 1-h period. Cofactors ATP and NADPH were regenerated via pyruvate kinase and glucose dehydrogenase. A mathematical model was constructed on the basis of the kinetics of the purified enzymes and the measured half-life times of the pathway intermediates. The model quantitatively predicted the system fluxes and metabolite concentrations. Relative enzyme concentrations were chosen such that half the carbon in the system was lost due to degradation of the thermolabile intermediates dihydroxyacetone phosphate, glyceraldehyde 3-phosphate and 1,3-bisphosphoglycerate, indicating that intermediate instability at high temperature can significantly affect pathway efficiency.

Database
The mathematical models described here have been submitted to the JWS Online Cellular Systems Modelling Database and can be accessed at http://jjj.mib.ac.uk/database/kouril/index.html. The investigation and complete experimental data set is available on the SEEK at https://seek.sysmo-db.org/investigations/51.

Abbreviations
BPG, 1,3-bis-phosphoglycerate; DHAP, dihydroxyacetone phosphate; EMP, Embden–Meyerhof–Parnas; FBPA/ase, fructose 1,6-bisphosphate aldolase/phosphatase (EC 4.1.2.13); F6P, fructose 6-phosphate; GAP, glyceraldehyde 3-phosphate; GAPDH, glyceraldehyde 3-phosphate dehydrogenase (phosphorylating) (EC 1.2.1.12); GAPN, non-phosphorylating GAPDH; GAPOR, ferredoxin-dependent glyceraldehyde 3-phosphate oxidoreductase; G6P, glucose 6-phosphate; IPTG, isopropyl thio-β-D-galactopyranoside; PEP, phosphoenolpyruvate. 3-PG, 3-phosphoglycerate; PGK, phosphoglycerate kinase (EC 2.7.2.3); TPI, triose-phosphate isomerase (EC 5.3.1.1).

Introduction

Thermophilic organisms, mostly found among the Archaea and Bacteria domains, live at temperatures between 60 and 80 °C. In these organisms metabolic processes and specific biological functions have been adapted to these extreme conditions [1]. In the past, focus was mainly on the structural stability of macromolecules such as proteins, DNA and membranes at high temperatures [1–3]. However, life at high temperatures also requires adaptations to metabolism to cope with the influence of heat on small molecules such as metabolites and cofactors.

Thermal instability of metabolites can lead to loss of free energy and carbon or to the accumulation of dead-end compounds [4]. Possible strategies to handle this challenge include substrate channelling or the use of pathways without thermolabile intermediates. Analyses of intermediates of the central carbohydrate metabolic pathways showed that especially triose phosphates, such as glyceraldehyde 3-phosphate (GAP), dihydroxyacetone phosphate (DHAP) and 1,3-bisphosphoglycerate (BPG), with half-life times at 80 °C of the order of minutes, are unstable at high temperature [5–7]. The occurrence of unusual enzymes found in (hyper)thermophiles like the non-phosphorylating glyceraldehyde 3-phosphate dehydrogenase (GAPN), ferredoxin-dependent glyceraldehyde 3-phosphate oxidoreductase (GAPOR) and the anabolic, bifunctional fructose 1,6-bisphosphate aldolase/phosphatase (FBPA/ase) has been discussed previously as a special adaptation to life at high temperature [7–14]. However, so far experimental evidence is missing that the instability of metabolites can lead to severe carbon loss.

Sulfolobus solfataricus is a thermo-acidophilic crenarchaeon that grows optimally at 80 °C and pH 2–4 [15]. For glycolysis this model organism uses the modified branched Entner–Doudoroff pathway, while the Embden–Meyerhof–Parnas (EMP) pathway is used for gluconeogenesis [12,16–20]. *S. solfataricus* lacks a glycolytic 6-phosphofructokinase homologue, thereby limiting the role of the upper branch of the EMP pathway to gluconeogenesis [21].

Under gluconeogenic conditions pyruvate is metabolized to fructose 6- phosphate (F6P) via the lower branch of the EMP pathway, with phosphoenolpyruvate (PEP) synthetase bypassing the pyruvate kinase reaction. PEP is converted to 2-phosphoglycerate and further to 3-phosphoglycerate (3-PG) via phosphoglycerate mutase [22] and enolase. 3-PG is further metabolized via the glyceraldehyde 3-phosphate dehydrogenase (GAPDH)/phosphoglycerate kinase (PGK) couple [23–25]. Triosephosphate isomerase (TPI) catalyses the interconversion of GAP and DHAP and the bifunctional FBPA/ase catalysing the direct conversion of DHAP and GAP to F6P [13,26,27]. The FBPA/ase is unique for Archaea and deep branching bacteria and the enzyme has been suggested to be important for the rapid conversion of the heat-unstable triosephosphates GAP and DHAP to F6P [13]. F6P can be converted either via the reversed ribulose monophosphate pathway to pentoses, or via glucose 6-phosphate (G6P) to glycogen [28] or trehalose [21,29–31].

In this study we focus on the consequences of thermal instability of the EMP pathway intermediates DHAP, GAP and BPG for the efficiency of conversion of 3-PG to F6P in *S. solfataricus*. For this we cloned, purified and kinetically characterized four enzymes involved in gluconeogenesis, and we reconstituted the enzymes *in vitro* to study the pathway characteristics. These enzymes PGK, GAPDH, TPI and FBPA/ase constitute a minimal system that contains three thermolabile intermediates and thus produces a system with which we can test the extent of carbon loss due to

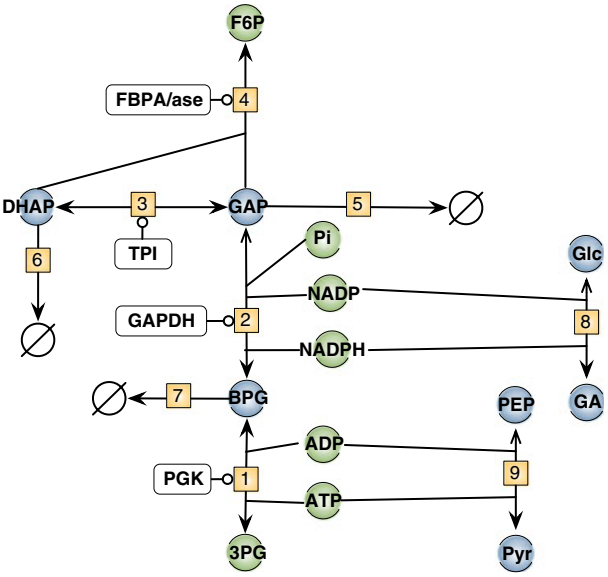

Fig. 1. Schema for the metabolic network. BPG, GAP and DHAP are variables of the system; 3-PG, NADP(H), AT(D)P and F6P are parameters for the minimal steady state model (i.e. considered as external metabolites for the system) but are modelled as variables in the extended model. Reactions 1, 2, 3 and 4 are the enzyme catalysed reactions (PGK, phosphoglycerate kinase; GAPDH, glyceraldehyde 3- phosphate dehydrogenase; TPI, triosephosphate isomerase; FBPA/ase, fructose 1,6-bisphosphate aldolase/phosphatase). Processes 5, 6 and 7 indicate the temperature degradation of GAP, DHAP and BPG respectively. Processes 8 (glucose dehydrogenase) and 9 (pyruvate kinase) are added to the extended model for cofactor regeneration.

thermal instability. Of course carbon is not really lost; in this study we define carbon loss as carbon disappearing from the network structure in which we work, i.e. carbon not present in the form 3-PG, BPG, GAP, DHAP or F6P. A detailed kinetic model for the system is constructed and validated with *in vitro* experiments. The extent of carbon loss in the *in vitro* system is significant and could easily add up to 50% of the carbon flow.

Results

Enzyme kinetics

We studied a part of the gluconeogenic pathway in *S. solfataricus* that contains three thermolabile intermediates (BPG, GAP and DHAP) from 3-PG to F6P at 70 °C. This pathway consists of four enzymes, PGK, GAPDH, TPI and FBPA/ase (see Fig. 1). We kinetically characterized the enzymes and made a detailed mathematical model for the pathway, including the thermal instability of the intermediates. For each reaction we used an enzyme kinetic rate equation that was derived on the basis of a biochemical mechanism (see Doc. S1) that sufficiently describes the enzyme kinetic data.

Heterologous gene expression and purification of the recombinant proteins

To characterize the proteins FBPA/ase, TPI, GAPDH and PGK, the respective genes were cloned and the proteins were expressed in *Escherichia coli*. The recombinant proteins were purified to apparent homogeneity by heat treatment at 80 °C for 20 min, followed by anion exchange and gel filtration chromatography. The molecular mass of the recombinant proteins estimated by SDS/PAGE agreed with that calculated from the deduced amino acid sequence

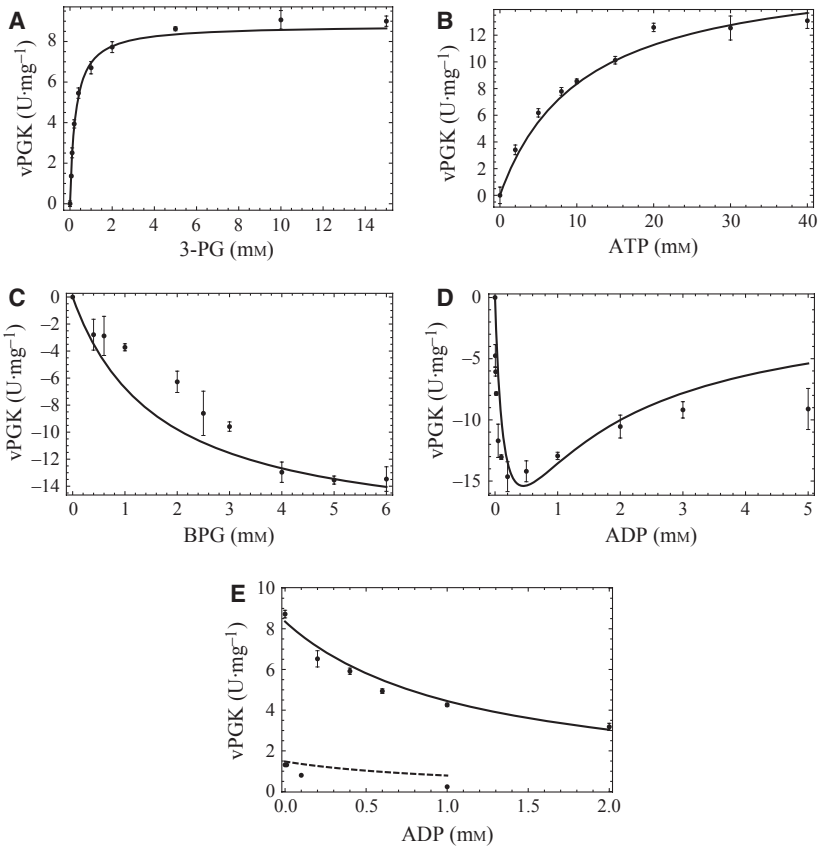

Fig. 2. PGK activity as a function of its substrate and product concentrations. The conversion of 3-PG to BPG is chosen as the forward direction of the enzyme (positive rate). (A) 3-PG saturation curve (10 mM ATP). (B) ATP saturation curve (5 mM 3-PG). (C) BPG saturation curve (0.2 mM ADP). BPG is unstable and not commercially available; for its analysis we varied GAP concentrations in a GAPDH linked assay. (D) ADP saturation curve (5 mM BPG). (E) ADP inhibition of the forward direction (5 mM 3-PG and 1 mM ATP, dashed line; or 10 mM ATP, solid line). The drawn line is the best fit of the rate equation (Eqn 1) to all data points. Error bars for data points denote the standard deviation; measurements were performed in triplicate.

(FBPA/ase 43 kDa; TPI 25 kDa; GAPDH 38 kDa, PGK 45 kDa).

Phosphoglycerate kinase

PGK catalyses the reversible reaction 3-PG + ATP ↔ BPG + ADP. We characterized the enzyme with respect to substrate and product saturation for the forward and backward activities at 70 °C. The enzyme showed hyperbolic saturation kinetics for 3-PG, ATP and BPG (Fig. 2A,B,C) but for ADP it showed more complicated kinetics: a high affinity binding for the reaction in the reverse direction and a low affinity inhibitory effect for the forward as well as the reverse reaction (Fig. 2D,E). To derive a rate equation for the enzyme we assumed an ordered mechanism where 3-PG and BPG bind before ADP and ATP. In addition we assumed that ADP can bind with low affinity ($K_{i,ADP}$) to all enzyme forms. This mechanism leads to the following rate equation:

$$v_{PGK} = \frac{V_{Mf}\cdot\frac{ATP\cdot 3PG}{K_{M,ATP}\cdot K_{M,3PG}} - V_{Mr}\cdot\frac{ADP\cdot BPG}{K_{M,ADP}\cdot K_{M,BPG}}}{(1+\frac{ADP}{K_{i,ADP}})\{1+\frac{3PG}{K_{M,3PG}}(1+\frac{ATP}{K_{M,ATP}})+\frac{BPG}{K_{M,BPG}}(1+\frac{ADP}{K_{M,ADP}})\}} \quad (1)$$

with ATP, ADP, 3PG and BPG concentrations of the respective metabolites, K_M binding constants for reactants and products, K_i binding constants for inhibitors, V_{Mf} and V_{Mr} the maximal rate in the forward and reverse direction respectively. Fitting this rate equation to the experimental data points (shown in Fig. 2) resulted in the parameter values shown in Table 1. For parameter estimation an objective function based on the sum of squared differences for all data sets and the rate equation was minimized.

ADP bound much more strongly to the adenine nucleotide binding site of the PGK than ATP (Fig. 2B, D); at high ADP concentration an inhibitory effect in both forward and reverse direction was observed (Fig. 2D,E). The low affinity of the enzyme for BPG is most probably influenced by the assay method. In the assay, we assumed a complete and immediate conversion of GAP to BPG based on the addition of saturating GAPDH to the incubation (see Materials and methods for details). Most probably the actual concentration of BPG in the assay will be lower, leading to an overestimation of the $K_{M,BPG}$ value for PGK. The data set did not allow for a precise determination of $K_{M,BPG}$.

Glyceraldehyde 3-phosphate dehydrogenase

GAPDH catalyses the reversible reaction BPG + NADPH ↔ GAP + $NADP^+$ + P_i. We characterized the enzyme with respect to substrate and product saturation for the forward and backward activities. The enzyme showed hyperbolic saturation kinetics for NADPH and $NADP^+$ (Fig. 3B,D) but showed sigmoidal saturation kinetics for BPG, GAP and P_i (Fig. 3A,C,E). We assumed a reversible Hill equation with two substrates and three products [32,33], assuming cooperativity for the GAP, BPG and P_i binding sites. This leads to the following rate equation:

$$v_{GADPH} = \frac{(\frac{V_{Mf}\cdot BPG\cdot NADPH}{K_{M,BPG}\cdot K_{M,NADPH}} - \frac{V_{Mr}\cdot GAP\cdot NADP\cdot P_i}{K_{M,GAP}\cdot K_{M,NADP}\cdot K_{M,P_i}})\cdot(\frac{GAP\cdot P_i}{K_{M,GAP}\cdot K_{M,P_i}}+\frac{BPG}{K_{M,BPG}})^{(n-1)}}{(1+\frac{NADP}{K_{M,NADP}}+\frac{NADPH}{K_{M,NADPH}})\{1+(\frac{GAP}{K_{M,GAP}})^n+(\frac{P_i}{K_{M,P_i}})^n+(\frac{GAP\cdot P_i}{K_{M,GAP}K_{M,P_i}}+\frac{BPG}{K_{M,BPG}})^n\}} \quad (2)$$

This equation was fitted to the experimental data points shown in Fig. 3, resulting in the parameter values listed in Table 2. The GAPDH showed much higher affinities for its substrates BPG and NADPH than for its products GAP, P_i and $NADP^+$. Specifically the low affinity for P_i ($K_{M,Pi}$ = 409 mM) would severely limit the activity of the enzyme in its catabolic direction under physiological conditions. Since we could not attain saturating [P_i] in the assay, we used arsenate (300 mM) for the binding studies of the other substrates and products.

Triose-phosphate isomerase

TPI catalyses the reversible reaction GAP ↔ DHAP. The enzyme showed hyperbolic saturation kinetics for its substrate and product (Fig. 4A,B) and strong inhibition by 3-PG and PEP (data not shown). We modelled the reaction with a reversible Michaelis–Menten equation with 3-PG and PEP as competitive inhibitors (Eqn 3).

$$v_{TPI} = \frac{V_{Mf}\cdot\frac{GAP}{K_{M,GAP}} - V_{Mr}\cdot\frac{DHAP}{K_{M,DHAP}}}{(1+\frac{GAP}{K_{M,GAP}}+\frac{DHAP}{K_{M,DHAP}}+\frac{3PG}{K_{i,3PG}}+\frac{PEP}{K_{i,PEP}})} \quad (3)$$

Table 1. Parameter values for the PGK reaction, determined at 70 °C. The parameter values were obtained by fitting Eqn (1) to the experimental data shown in Fig. 2. For assay conditions see Materials and methods.

V_{Mf} (U·mg^{-1})	V_{Mr} (U·mg^{-1})	$K_{M,ATP}$ (mM)	$K_{M,ADP}$ (mM)	$K_{i,ADP}$ (mM)	$K_{M,P3G}$ (mM)	$K_{M,BPG}$ (mM)
17.32	30.04	9.685	0.085	1.142	0.541	5.590

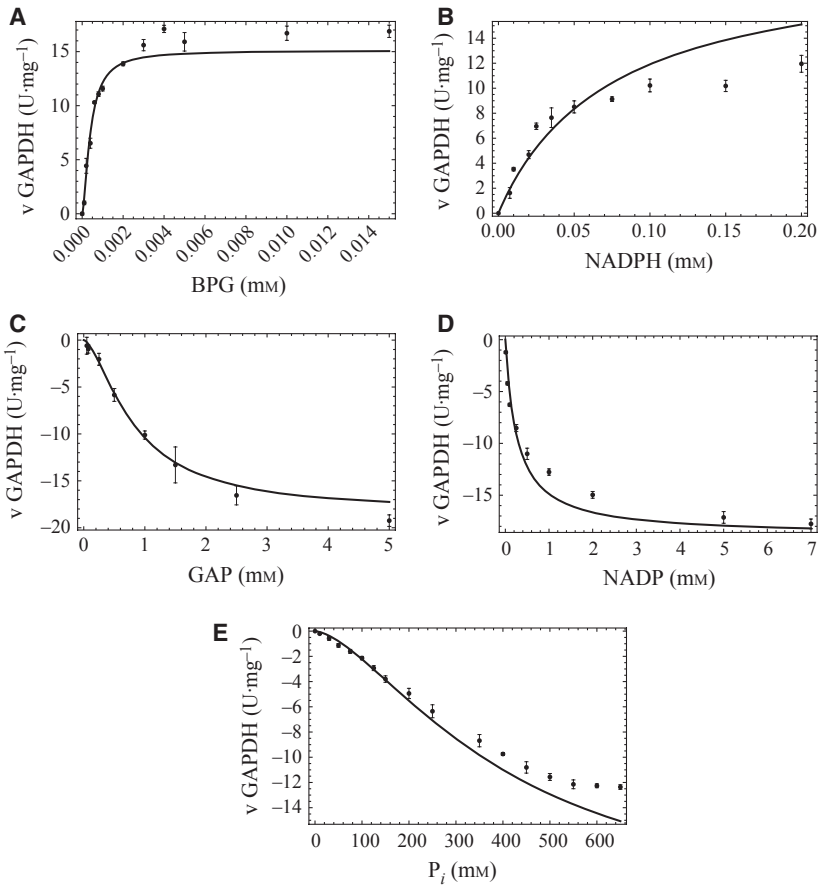

Fig. 3. GAPDH activity as a function of its substrate and product concentrations, at 70 °C. The conversion of BPG to GAP was chosen as the forward direction of the enzyme (positive rate). The drawn line is the best fit of the rate equation (Eqn 2) to all data points. Standard assay conditions (see Materials and methods) were chosen for the metabolite concentrations that were not varied. BPG is unstable and not commercially available; we could only vary its concentration indirectly by changing 3-PG concentrations in a PGK linked assay. Error bars denote the standard deviation; measurements were performed in triplicate.

Fitting this equation to the experimental data points resulted in the enzyme kinetic parameters listed in Table 3. The enzyme has a slightly higher affinity for GAP than for DHAP, and its maximal rate (per milligram purified protein) is much higher than that of PGK, GAPDH and FBPA/ase.

Fructose 1,6-bisphosphate aldolase/phosphatase

FBPA/ase is a bifunctional enzyme that catalyses two consecutive steps in the anabolic (gluconeogenic) pathway, namely the aldolase reaction DHAP + GAP ↔ FBP and the irreversible hydrolysis FBP → F6P + P_i. The enzyme uses DHAP and GAP or alternatively FBP as substrate. Under the conditions tested the overall reaction DHAP + GAP → F6P + P_i is irreversible and FBP is not released from the FBPA/ase. Saturation curves for DHAP and GAP were determined for the combined reactions. Since we analyse the system in a linked assay it was not possible to study F6P inhibition. The enzyme showed hyperbolic saturation curves for both substrates.

Table 2. Parameter values for the GAPDH reaction, determined at 70 °C. The parameter values were obtained by fitting Eqn (2) to the experimental data shown in Fig. 3. For assay conditions see Materials and methods.

V_{Mf} (U·mg^{-1})	V_{Mr} (U·mg^{-1})	$K_{M,BPG}$ (mM)	$K_{M,NADPH}$ (mM)	$K_{M,NADP}$ (mM)	$K_{M,Pi}$ (mM)	$K_{M,GAP}$ (mM)	n
20.6526	24.054	0.00041	0.074	0.271	408.5	0.838	1.56

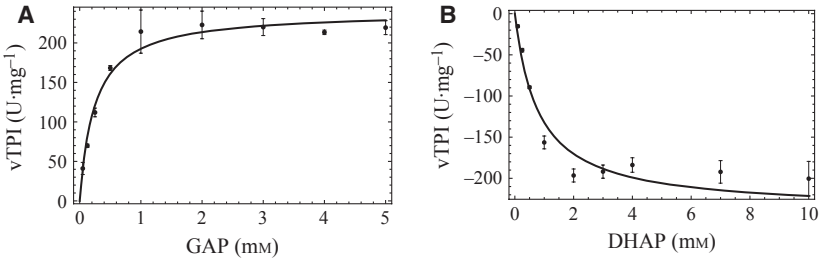

Fig. 4. TPI activity as a function of its substrate and product concentrations. The forward direction of the enzyme is chosen as the conversion of GAP to DHAP (positive rate). The drawn line is the best fit of the rate equation (Eqn 3) to all data points. Standard assay conditions (see Materials and methods) were chosen for the metabolite concentrations that were not varied. Error bars denote the standard deviation; measurements were performed in triplicate.

Table 3. Parameter values for the TPI reaction, determined at 70 °C. The parameter values were obtained by fitting Eqn (3) to the complete kinetic data set for TPI. For assay conditions see Materials and methods.

V_{Mf} (U·mg^{-1})	V_{Mr} (U·mg^{-1})	$K_{M,GAP}$ (mM)	$K_{M,DHAP}$ (mM)	$K_{i,P3G}$ (mM)	$K_{i,PEP}$ (mM)
240.0	239.4	0.245	0.812	0.400	0.661

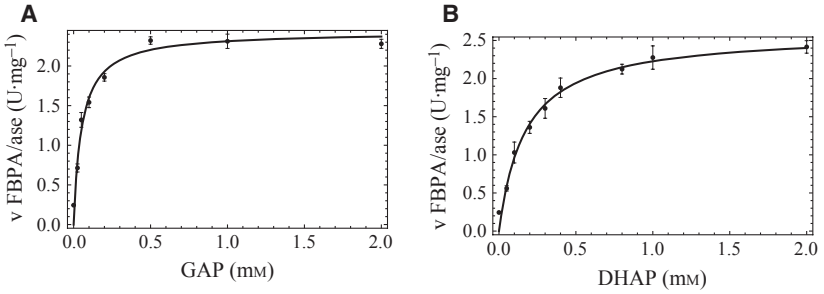

Fig. 5. FBPA/ase activity as a function of its substrate concentration, at 70 °C. The forward direction of the enzyme is chosen as the conversion of GAP + DHAP to F6P (positive rate). The drawn line is the best fit of the rate equation (Eqn 4) to all data points. For the GAP saturation reaction 2 mM of DHAP was chosen and for the DHAP saturation 2 mM of GAP was chosen; see Materials and methods for the assay conditions. Error bars denote the standard deviation; measurements were performed in triplicate.

Table 4. Parameter values for the FBPA/ase reaction, determined at 70 °C. The parameter values were obtained by fitting Eqn (4) to the experimental data shown in Fig. 5. For assay conditions see Materials and methods.

V_{Mf} (U·mg^{-1})	$K_{M,GAP}$ (mM)	$K_{M,DHAP}$ (mM)
2.64	0.052	0.171

The reaction was described with a random order binding mechanism for an irreversible-product-insensitive two-substrate model:

$$v_{\mathrm{FBPA/ase}} = \frac{V_{\mathrm{Mf}} \cdot \frac{GAP}{K_{\mathrm{M,GAP}}} \cdot \frac{DHAP}{K_{\mathrm{M,DHAP}}}}{\left(1 + \frac{GAP}{K_{\mathrm{M,GAP}}} + \frac{DHAP}{K_{\mathrm{M,DHAP}}} + \frac{GAP \cdot DHAP}{K_{\mathrm{M,GAP}} K_{\mathrm{M,DHAP}}}\right)} \quad (4)$$

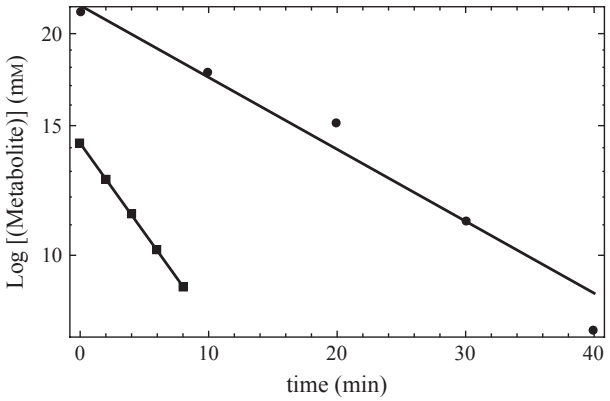

Fig. 6. Degradation of DHAP and GAP at 70 °C. DHAP (circles) and GAP (squares) were incubated in the assay buffer at 70 °C and concentration changes were measured over time. The lines show the fitted exponential decay functions.

Fitting this equation to the experimental data points (Fig. 5) resulted in the enzyme kinetic parameters listed in Table 4.

Non-enzymatic degradation

Half-life times for GAP and DHAP of 12.4 and 30.8 min were measured at 70 °C in the incubation buffer (Fig. 6). BPG is not commercially available and we assumed a half-life time of 0.655 min, which is calculated from the literature value of 1.6 min at 60 °C [6] assuming similar changes in half-life of BPG upon increasing the temperature from 60 to 70 °C as were measured for DHAP and GAP. These half-life times lead to kinetic constants for degradation of intermediates k_{deg} of 1.058, 0.056 and 0.023 min^{-1} for BPG, GAP and DHAP, respectively.

The change in concentration of the intermediates due to temperature degradation can be described by mass action kinetics:

$$v_{\mathrm{deg}}X = k_{\mathrm{deg}}X \cdot X \tag{5}$$

with X any of the three temperature-sensitive intermediates.

Network reconstitution

The simplest network that contains the three most thermolabile intermediates (BPG, GAP and DHAP) consists of the four enzymes that were isolated and characterized: PGK, GAPDH, TPI and FBPA/ase. Together these enzymes catalyse the conversion of 3-PG to F6P (see Fig. 1). After a number of trial experiments and model simulations we selected relative enzyme amounts for which we observed an equal contribution of the enzyme catalysed reactions and the temperature dependent, intermediate degradation reactions. These conditions are the best test conditions for the model and for characterizing the contribution of the temperature degradation of intermediates to the efficiency of carbon conversion at high temperature. They do not necessarily reflect the exact conditions as observed in the intact cell; this will be addressed in a future work. Here we were interested in testing whether the temperature sensitivity of the pathway intermediates can contribute significantly to the efficiency of carbon conversion in the gluconeogenic pathway.

The relative amounts for the PGK, GAPDH, TPI and FBPA/ase used in the study were 0.08 : 1 : 0.02 : 0.09. Following these ratios, a total concentration of 50 $\mu\mathrm{g}\cdot\mathrm{mL}^{-1}$ of purified proteins was used to reconstitute the *in vitro* system. To maintain high ratios of cofactors (ATP/ADP, NADPH/NADP^{+}) purified pyruvate kinase and glucose dehydrogenase were added to the reconstituted system (see Materials and methods for assay details). Initial assay conditions were 10 mM ATP, 2 mM 3-PG and 0.2 mM NADPH (with 5 mM PEP and 10 mM glucose; no pyruvate and gluconate was present at $t = 0$).

In the reconstituted system a constant 3-PG consumption rate and F6P production rate of −0.026 mM 3-PG·min^{-1} and 0.0055 mM F6P·min^{-1} were observed over a 1-h period, during which the intermediates peaked at 0.15 mM for GAP and 0.2 mM for DHAP. In total 0.55 mM of F6P is formed from the initial 2.0 mM 3-PG. BPG was only present at very low concentration, i.e. below 0.06 μM. Pyruvate production rate (reflecting the ATP recycling) is close to the 3-PG consumption rate: 0.024 mM pyruvate per minute. During the incubation [ADP] remained low at 0.02 mM (± 0.01 mM), indicating that the recycling system was effective.

Model construction

The network structure for the model consists of the four enzymes that were isolated, characterized and reconstituted: PGK, GAPDH, TPI and FBPA/ase. The combined reactions lead to the following set of ordinary differential equations:

$$\frac{dBPG}{dt} = v_{\mathrm{PGK}} \cdot [PGK] - v_{\mathrm{GAPDH}} \cdot [GAPDH] - v_{\mathrm{degBPG}} \tag{6}$$

$$\frac{dGAP}{dt} = v_{\mathrm{GAPDH}} \cdot [GAPDH] - v_{\mathrm{TPI}} \cdot [TPI] - v_{\mathrm{FBPA/ase}} \cdot [FBPA/ase] - v_{\mathrm{degGAP}} \tag{7}$$

$$\frac{dDHAP}{dt} = v_{\mathrm{TPI}} \cdot [TPI] - v_{\mathrm{FBPA/ase}} \cdot [FBPA/ase] - v_{\mathrm{degDHAP}} \quad (8)$$

with the respective rate equations for the enzymes given in Eqns (1–4) with parameter values given in Tables 1–4, multiplied by their respective enzyme concentrations. For the non-enzymatic degradation the mass action kinetics given in Eqn (5) were used with the kinetic constants given in the section Non-enzymatic degradation.

Model validation

A steady state analysis of the kinetic model for the boundary conditions 2 mM 3-PG, 10 mM ATP, 0.2 mM NADPH, 5 mM PEP and zero concentrations for the other external parameters resulted in a steady state for which the fluxes were close to the experimentally observed values: 0.026 mM 3-PG consumed per minute and 0.004 mM F6P produced per minute. The steady state intermediate concentrations were 0.23 mM GAP, 0.22 mM DHAP and 0.059 μM BPG. The model can be analysed on line at http://jjj.mib.ac.uk/webMathematica/UItester.jsp?modelName=kouril2. Sensitivity analyses for small changes in all parameter values of the model and for large changes in the relative enzyme concentrations are given in Doc. S1.

In the experimental incubation of the four enzymes no true steady state was reached; although the consumption rate of 3-PG and the production rate of F6P were constant for a 1-h period, both GAP and DHAP showed an optimum in their concentration, followed by a gradual decrease (Fig. 7). To simulate a time course for the conversion of 3-PG to F6P with the concomitant changes in intermediate levels we extended the three-variable model to include 3-PG and F6P as variables. In addition, we modelled the cofactors and their regeneration via the pyruvate kinase and glucose dehydrogenase system.

This extended kinetic model predicts the experimental data set precisely in terms of fluxes (Fig. 7A) and intermediate concentrations (Fig. 7B). The shaded areas in Fig. 7 denote the ranges for metabolite concentrations when a 5% error is allowed in the model parameters. The model can be analysed on line at http://jjj.mib.ac.uk/webMathematica/UItester.jsp?modelName=kouril3.

The initially low DHAP/GAP ratio becomes greater than 1 only after approximately 40 min. This was unexpected since the high activity of the enzyme would always ensure a DHAP/GAP ratio higher than 1. On the basis of model simulations we predicted that TPI was inhibited strongly at the beginning of the incubation, which was experimentally confirmed by the inhibition of 3-PG and PEP. In the reconstituted system the concentrations of these metabolites are high initially and decrease gradually over time (at t = 80 min both inhibitor concentrations are very low and the DHAP/GAP ratio approaches the apparent K_{eq} value of TPI of 3.3, as calculated with the Haldane equation with parameter values from Table 3).

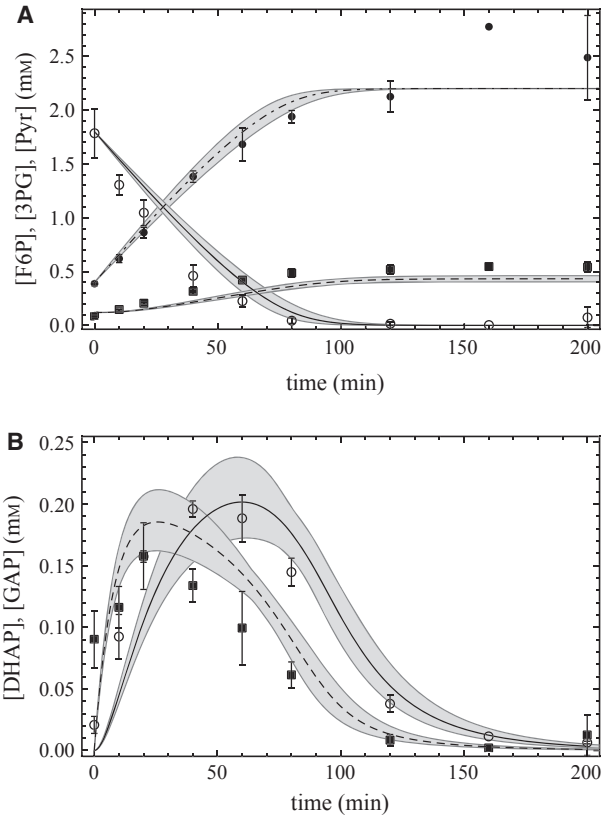

Fig. 7. Conversion of 3-PG to F6P in the reconstituted system. Experimental data (symbols) and model predictions (lines) for external metabolite concentrations [A, 3-PG (open circles, solid line), F6P (solid squares, dashed line) and pyruvate (solid circles, dot-dash line)] and intermediate metabolite concentrations [B, GAP (solid squares, dashed line) and DHAP (open circles, solid line)] are shown as a function of time. The shaded areas indicate the ranges of metabolite concentrations that were obtained in model simulations where parameter values were allowed to vary by ±5% of their measured values (see Computational methods for details). BPG was below detection limits throughout the experiment. Experiments were performed in triplicate; error bars denote the standard deviation.

Discussion

The high environmental temperatures in the natural habitat of *S. solfataricus* cause a serious threat in terms of carbon loss due to thermal instability of pathway intermediates. Whereas the stability of macromolecular

structures such as proteins, membranes, DNA and RNA has been considered extensively, relatively little attention has been given to the stability of low molecular weight molecules such as metabolic pathway intermediates. In this study we considered the contribution of the temperature sensitivity of three thermolabile intermediates in an *in vitro* reconstituted system of a central carbon metabolic pathway, gluconeogenesis.

The three most labile compounds in glycolysis are BPG, GAP and DHAP and we constructed a minimal system that comprises these three intermediates with the heat-stable external metabolites 3-PG and F6P. The four enzymes that form this system were kinetically characterized and a mathematical model was constructed to describe the dynamics of the system. The model also included the kinetic degradation of the thermolabile compounds. None of the model parameters was adapted from their experimentally determined values and as such the model gives a true prediction of the system's behaviour as a function of the characteristics of the isolated enzymes.

In the kinetic analysis of the gluconeogenic enzymes some of the K_M values showed non-physiologically high values for metabolites that would function as substrates in the catabolic direction of the pathway, i.e. K_M for phosphate for the GAPDH and K_M for BPG for the PGK. However, it should be noted that the K_M of BPG is most probably strongly overestimated due to our assumption that the surplus of added GAPDH in the linked assay converts GAP immediately and quantitatively into BPG. These high K_M values (compared with expected *in vivo* concentrations of substrates) indicate that the PGK and GAPDH play a more important role in gluconeogenesis than in glycolysis in *S. solfataricus*. To bypass the GAPDH/PGK reactions in the catabolic direction, GAPN has been proposed as the more important enzyme in *S. solfataricus* [11].

A kinetic study of the recombinant *Sulfolobus tokodaii* GAPDH revealed that this enzyme also exhibits higher activity in the gluconeogenic direction than in the glycolytic direction [34]. The physiological roles of GAPN, GAPOR, GAPDH and PGK have been analysed by constructing gene disruption strains of *Thermococcus kodakarensis* with subsequent monitoring of their growth phenotypes under glycolytic and gluconeogenic conditions [14]. Disruption of either GAPN or GAPOR did not affect gluconeogenic growth of *T. kodakarensis*, whereas no growth was observed under glycolytic conditions in these disruption strains. In contrast, experiments with GAPDH and PGK disruption strains displayed growth similar to that of the host strain under glycolytic conditions and no growth under gluconeogenic conditions. Taken together, these studies underline the importance of GAPN and GAPOR in glycolysis and of the GAPDH/PGK couple in gluconeogenesis in (hyper)thermophiles. The FBPA/ase is irreversible and will only be active in gluconeogenesis while the TPI is an enzyme that is usually close to equilibrium, i.e. can function equally well in both directions.

In this study a close agreement was obtained for the experimentally measured fluxes and intermediate concentrations and the model predictions. On the basis of this close agreement we conclude that the model can be used as a tool to calculate the contribution of thermodegradation to the overall pathway efficiency. This might appear to be an indirect method, but since the degradation products of the thermolabile compounds are not known and could very well be pathway intermediates, an analysis on the basis of experimental measurements only would be difficult, and we used the mathematical model as an additional analysis tool.

In the reconstituted system, constant 3-PG consumption and F6P production rates were observed during the first hour of the incubation, after which the system runs out of 3-PG. In a minimal model (with clamped 3-PG and F6P concentrations) a steady state is reached with similar fluxes: -0.026 mM 3-PG consumed per minute and 0.004 mM F6P produced per minute for the model prediction, and -0.026 mM 3-PG·min^{-1} and 0.0055 mM F6P·min^{-1} for the experimentally measured values.

For the complete progression curve for conversion of substrate to product, a total of 2.0 mM 3-PG is converted into 0.55 mM F6P in the experiment (and to 0.45 mM F6P in the model simulation), indicating an efficiency of 55% (and 45% for the model simulation). In Fig. 8 the total carbon content in the system, calculated as carbon content in 3-PG, F6P, GAP and DHAP ([BPG] is negligibly small), is calculated for each of the time points during the conversion of 3-PG to F6P.

The conversion of 3-PG to F6P is predicted closely by the model, which is based on experimentally measured parameter values for each of the isolated reaction steps, and was not fitted to the four enzyme system data. On the basis of this close agreement between model and experiment we conclude that the low efficiency of carbon conversion from 3-PG to F6P is due to thermal instability of BPG, GAP and DHAP.

The reference state was chosen such that approximately 50% of the carbon was lost due to thermal instability of the pathway intermediates, and the relative enzyme concentrations in this reference state do not necessarily reflect physiological conditions. To test the sensitivity of the carbon conversion efficiency for large changes in relative enzyme concentrations we varied the concentrations of PGK, TPI and FBPA/ase

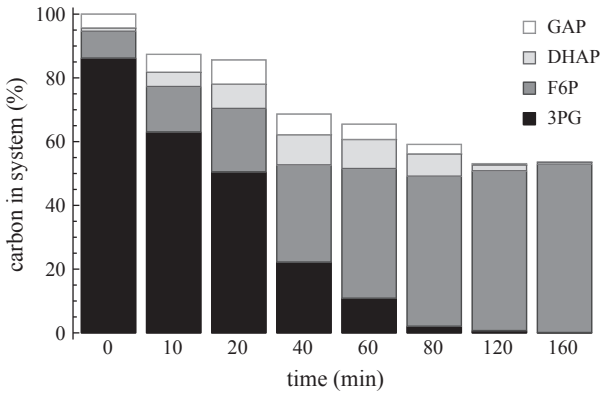

Fig. 8. Total carbon in the reconstituted system during 3-PG conversion. For each of the samples taken during the 3-PG conversion experiment the total carbon content in the 3-PG, F6P, GAP and DHAP pools was calculated as a percentage of the initial carbon content ([BPG] is negligibly small). After complete conversion of 3-PG only 55% of the initial carbon is retrieved as F6P.

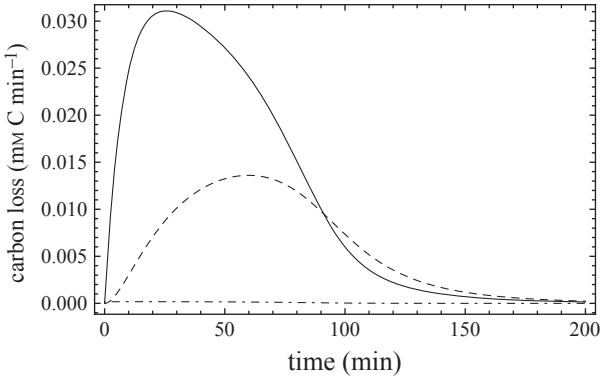

Fig. 9. Carbon loss from the reconstituted gluconeogenic system during 3-PG conversion. The (model predicted) degradation rate during the 3-PG conversion experiment (Fig. 7) is shown for each of the three thermolabile intermediates (solid line, GAP degradation rate; dashed line, DHAP degradation rate; dot-dashed line, BPG degradation rate).

between 0% and 500% of the reference state, while keeping the total protein concentration at 50 $\mu g \cdot mL^{-1}$ by adjusting the GAPDH accordingly. Running sufficient simulations for the solution to converge we obtained a mean carbon efficiency of 39.5% with a standard deviation of 20.5%. The minimal and maximal efficiency were 0% and 76% respectively. Thus irrespective of the relative enzyme concentrations a significant percentage of the carbon was lost due to thermal instability of the pathway intermediates.

Although BPG is the most unstable intermediate, it does not contribute strongly to the carbon loss as it has a very low concentration (experimental measurement and model estimate for maximal BPG concentration is 0.06 μM). The biggest contribution to carbon loss is via GAP and DHAP decay (Fig. 9).

Although the current *in vitro* reconstruction of gluconeogenesis does not necessarily reflect *in vivo* conditions, our study represents the first proof that thermal degradation of intermediates can significantly influence pathway efficiency and might represent a major challenge for life at high temperature. It is tempting to speculate that unique (hyper)thermophilic Archaea enzymes, such as gluconeogenic FBPA/ase, glycolytic GAPN and GAPOR, and the suggested restriction of the GAPDH/PGK enzyme couple for gluconeogenic function only, represent special adaptations to minimize carbon loss via thermal degradation.

An organism cannot change the thermal stability of the intermediates in a given pathway, but different strategies can be followed for the regulation of pathway fluxes. Clearly, strategies that would minimize pathway intermediate concentrations would be beneficial for increasing the pathway efficiency. Similarly one can envision that an increased ratio of flux to efficiency can be obtained by increasing total protein levels in a given metabolic system. At present we are investigating different regulatory strategies for the cell to increase gluconeogenic fluxes while not compromising the efficiency of the pathway too much. The *in vitro* system we have developed in this study gives us a tool to quantify the contribution of different suggested mechanisms to the metabolic adaptations at high temperature.

Conclusion

Here we report on a detailed kinetic characterization of four enzymes (PGK, GAPDH, TPI, FBPA/ase) involved in 3-PG to F6P conversion in *S. solfataricus*. A detailed mathematical model was constructed on the basis of these experimental data, which also included half-life times of pathway intermediates at high temperature (70 °C). Without further fitting, this model was tested in its ability to predict the dynamics of an *in vitro* reconstituted system of the four enzymes. Since the model is completely based on experimentally measured parameters, both for the enzyme kinetics and for the temperature sensitivity of GAP, DHAP and BPG, we conclude on the basis of the close agreement between model predictions and experimental results that the observed low efficiency of conversion is due to the temperature dependent degradation of GAP, DHAP and BPG. The carbon loss determined in the *in vitro* system as well as in the model reached 50–60% under the chosen assay conditions. These results demonstrate that the stability of pathway intermediates can be a major challenge for life at high temperature.

Table 5. List of primer sets, bacterial expression vectors and expression hosts. Recognition sites for restriction endonucleases are underlined.

Gene	bp	Primer (5′ → 3′)	Endonuclease	Plasmid	Host
SSO0286	1146	aldPaseF GGGGGAATTCATATGAAAACTACACTTAGTG	*Nde*I	pET11c	Rosetta(DE3)
aldPase		aldPaseR GGCGGGGATCCTCATTCATGTGAACTTTCGTG	*Bam*HI		
SS02592	681	tpiF GGGAATTCATATGAAACCTCCTATTATTATAATAAAC	*Nde*I	pET11c	Rosetta(DE3)
tpi		tpiR GGCGGGGATCCTCACGAAGAGATCGCCCTCAATGC	*Bam*HI		
SSO0528	1020	gapdhF GGGGGAATTCATGATTAATGTAGCTG	*Bsp*HI	pET324	BL21(DE3)RIL
gapdh		gapdhR GGCGGGGATCCTCATATTAGATACCCC	*Bam*HI		
SSO0527	1245	pgkF AAACCATGGATGGGGATCTTTCTGATTAAAGTG	*Nco*I	pET15b	BL21(DE3)
pgk		pgkR TTTCTCGAGTCAATCACCGCTATTCACCA	*Xho*I		

Materials and methods

Cloning of *S. solfataricus* genes *pgk, tpi, fbpA/ase* and *gapdh*

For the construction of the expression vectors, the coding regions were amplified from genomic DNA of *S. solfataricus* by PCR mutagenesis, using the primer sets given in Table 5. The amplified DNA fragments were cloned into pET expression vectors pET15b, pET11c (Agilent Technologies, Ratingen, NRW, Germany) using restriction endonucleases (Table 5). The sequences were confirmed by sequencing of both strands (LGC Genomics, Berlin, Germany).

Expression and purification of the recombinant enzymes

The *E. coli* strains were transformed with the resulting plasmids and *E. coli* strains BL21(DE3), BL21-CodonPlus (DE3)-RIL and Rosetta(DE3) (grown in the presence of 34 $\mu g \cdot mL^{-1}$ chloramphenicol) were cultivated at 37 °C in LB broth (Sigma-Aldrich, Taufkirchen, Germany). When an optical density (600 nm) of 0.6 was reached, overexpression was induced by adding 1 mM isopropyl thio-β-D-galactopyranoside (IPTG) (except for PGK expression, which was induced with 0.4 mM IPTG) to the medium. After 3–4 h of incubation with IPTG, the cells were harvested by centrifugation (6000 ***g***, 20 min, 4 °C) and resuspended (1 : 3) in 100 mM HEPES/KOH buffer (pH 7, room temperature; PGK, GAPDH) or 100 mM Tris/HCl (pH 7, room temperature; TPI, FBPA/ase), and cell disruption was carried out by ultrasonic treatment. In the case of PGK, TPI and GAPDH all buffers were supplemented with 10 mM dithiothreitol. After centrifugation (16 000 ***g***, 45 min, 4 °C), the soluble cell extract was heat treated for 20 min at 80 °C (GAPDH, FBPA/ase) or 70 °C (PGK) or 90 °C (TPI). The denatured host proteins were removed by centrifugation (16 000 ***g***, 30 min, 4 °C). The resulting supernatants were dialysed overnight using 20 mM HEPES/KOH (pH 7, room temperature) for PGK and GAPDH or 20 mM Tris/HCl (pH 7, room temperature) for TPI, FBPA/ase and subjected to ion exchange chromatography on UNO Q-12 (Bio-Rad Laboratories, München, Germany) or Resource Q (GE-Healthcare, Freiburg, Germany), equilibrated with the dialysis buffer. Elution proceeded using a continuous flow of the dialysis buffer with a linear gradient of NaCl from 0 M to 1 M. The pools of active fractions were combined and concentrated by the use of Vivaspin6 (Satorius, Göttingen, Germany) and then further purified by gel filtration (HiLoad 26/60 Superdex 200 prep grade, Amersham Biosciences, Glattbrugg, Switzerland) with a mobile phase of 50 mM HEPES/KOH (pH 7) for PGK and GAPDH or 50 mM Tris/HCl (pH 7, room temperature) for TPI, FBPA/ase, containing 0.3 M KCl (flow rate of 1 $mL \cdot min^{-1}$). During purification it was found that the FBPA/ase is an extremely unstable protein, losing 60% of its activity over 120 h after cell disruption; therefore 20 mM $MgCl_2$ was added to the buffers to stabilize the protein, as reported previously [13]. Due to its instability, the protein extract after heat precipitation was loaded on a gel filtration column (HiLoad 26/60 Superdex 200 prep grade, Amersham Biosciences) with 50 mM Tris/HCl, 300 mM NaCl, 20 mM $MgCl_2$ as mobile phase, and subsequently aliquots of the purified protein were stored in the presence of 20% glycerol (v/v) at −80 °C.

Kinetic assays

For measuring enzyme activities at high temperature we used linked assays to couple enzyme activity to NADH production or consumption. For this the production of (hyper)thermophilic auxiliary enzymes was necessary. In general, for enzyme assays, auxiliary enzymes were enriched via heat precipitation (see below) and provided in excess to ensure that they did not limit the enzyme velocity of the target enzymes. For each assay three independent measurements were performed with control reactions without substrate or enzyme, respectively, following an increase/decrease in absorbance at 340 nm in a Specord 210 photometer (Analytic Jena, Jena, Germany). Enzyme activities are expressed as $U \cdot mg^{-1}$ purified protein, i.e. μmol substrate $consumed \cdot min^{-1} \cdot mg^{-1}$ purified protein. Reactions were started by the addition of substrate. The D,L-glyceral-

dehyde 3-phosphate solution used for the characterization of GAPDH, TPI and FBPA/ase contained only 50% of the enzymatically active D-isomer (Sigma-Aldrich). For the enzyme assays we assumed that the L-isomer had no effect on the enzyme activity.

Expression and purification of (hyper)thermophilic auxiliary enzymes

Expression of the (hyper)thermophilic auxiliary enzymes phosphoglycerate kinase (Ttx-PGK), hexokinase (Ttx-HK) and glucose 6-phosphate isomerase (Ttx-PGI) from *Thermoproteus tenax* and *Thermotoga maritima* glucose 6-phosphate dehydrogenase (Tma-G6PDH) as well as glucose dehydrogenase (Sso-GDH), phosphoglycerate kinase (Sso-PK), GAPDH and GAPN from *S. solfataricus* was carried out in 2 L Erlenmeyer flasks containing 1 L LB medium (Sigma-Aldrich) at 37 °C and 180 rpm. The cells were cultivated, harvested and disrupted as described in the respective publications (Ttx-PGI [35]; Ttx-PGK [9]; Ttx- HK [36]; Tma-G6PDH [37]; Sso-GDH [38]; Sso-PK [39]; Sso-GAPN [11]) or for the PGK and GAPDH as described above. The cell-free extracts obtained were subjected to heat precipitation at 80 °C for 20 min and afterwards denatured proteins from the host were removed by centrifugation (16 000 ***g***, 30 min, 4 °C). Sso-GDH was further purified using ion exchange chromatography and gel filtration to apparent homogeneity [38]. Samples of the resulting supernatants were dialysed (Spectra/Por Dialyse Membrane, molecular weight cut-off 3.5 kDa; Spectrum Laboratories Inc., Compton, CA, USA) and directly used as auxiliary enzymes in enzyme assays or stored after addition of glycerol (20% v/v) at −80 °C.

FBPA/ase assay

A coupled enzyme assay was performed, using the Tma-G6PDH (4.6 μg after heat precipitation for 20 min at 80 °C) and the Ttx-PGI (7.6 μg of protein after heat precipitation for 20 min at 80 °C) as auxiliary enzymes, following the formation of NADPH at 340 nm. For the determination of K_M and V_{max} values, 7 μg FBPA/ase was incubated (500 μL total volume) in the presence of 100 mM Tris/HCl (pH 6.5, 70 °C), 20 mM $MgCl_2$, 1 mM $NADP^+$ and auxiliary enzymes and different concentrations of either D,L-GAP or DHAP (0–4 mM).

TPI assay

Catabolic TPI activities were assayed at 70 °C using the GAPN of *S. solfataricus* as auxiliary enzyme, i.e. a continuous assay for the conversion of DHAP to GAP. Each reaction was performed in 100 mM Tris/HCl (pH 6.5, 70 °C) containing 127 ng TPI (fresh 1 : 100 dilution after purification), 170 μg GAPN after heat precipitation (20 min at 80 °C) and 10 mM $NADP^+$ in a final volume of 500 μL. DHAP was added to start the reaction. In the anabolic direction assays were performed at 70 °C using the FBPA/ase, Ttx-PGI and Tma-G6PDH (protein solution after heat precipitation) as auxiliary enzymes. The reaction progress was followed via NADPH formation, measured spectrophotometrically at 340 nm. Each reaction was performed in 100 mM Tris/HCl, 20 mM $MgCl_2$ (pH 6.5, 70 °C), 50 μg FBPA/ase, 7.6 μg Ttx-PGI, 4.6 μg Tma-G6PDH and 1 mM $NADP^+$ in a final volume of 500 μL. Inhibition of TPI activity by 3-PG and PEP was measured in the catabolic direction only, using standard conditions and with varying 3-PG, PEP and DHAP concentrations.

GAPDH assay

Catabolic GAPDH activity was determined in a mixture contained 100 mM HEPES/KOH (pH 6.5, 70 °C), 300 mM sodium arsenate [40], 1.8 μg GAPDH and either varying concentrations of D,L-GAP (0–10 mM, 5 mM $NADP^+$) or varying concentrations of $NADP^+$ (0–7 mM, 10 mM D,L-GAP), essentially as described in [23]. Phosphate-dependent kinetics of GAPDH were determined in 100 mM HEPES/KOH (pH 6.5, 70 °C) with 1.8 μg GAPDH, at varying concentrations of KP_i (0–700 mM) in the presence of 5 mM $NADP^+$ and 10 mM D,L-GAP. In the anabolic direction a continuous, coupled enzyme assay was performed, using the Ttx-PGK as auxiliary enzyme (50 μg of protein solution after heat precipitation). The Ttx-PGK was provided in excess to ensure that most of the 3-PG was rapidly converted into BPG. The affinity of the enzyme for BPG, expressed as $K_{M,BPG}$, should only be considered an approximate value. For the determination of kinetic parameters 1.8 μg GAPDH was incubated in the presence of 20 mM $MgCl_2$, 5 mM ATP, 100 mM Tris/HCl (pH 6.5, 70 °C), 50 μg Ttx-PGK and different concentrations of either NADPH (0–200 μM, 6 mM 3-PG) or 3-PG (0–30 mM, 200 μM NADPH).

PGK assay

Anabolic PGK activity was measured in a continuous enzyme assay coupled with the oxidation of NADPH by GAPDH. The assay was performed at 70 °C in 0.1 M Tris/HCl (pH 6.5, 70 °C) containing 0.2 mM NADPH, 10 mM ATP, 10 mM $MgCl_2$, recombinant Sso-GAPDH (20 μg after heat precipitation) and 1.23 μg of purified PGK in a total volume of 500 μL at 340 nm. Reactions were started by the addition of 3-PG (final concentration 5 mM). Catabolic PGK activity was determined by following the amount of ATP formed. Since BPG is not commercially available it had to be synthesized by GAPDH during the assay. ATP was quantified using Ttx-HK and Tma-G6PDH (protein solutions after heat precipitation) in Tris/HCl (pH 6.5, 70 °C) buffer containing 5 mM $NADP^+$, 5 mM glucose, 0.4 M KP_i (pH 7), 20 mM $MgCl_2$, 5 mM ADP, 2 μg of GAPDH (protein solution after heat precipi-

tation) and 1 μg purified PGK (500 μL total volume). The assay was started by the addition of D,L-GAP. This assay was used for the determination of kinetic parameters in the presence of 0–5 mM ADP or 0–6 mM D,L-GAP and fixed concentrations of 5 mM D,L-GAP or 0.2 mM ADP, respectively. The ADP inhibition of anabolic PGK activity was determined in the presence of 10 mM or 1 mM ATP, respectively, 20 mM $MgCl_2$, 0.2 mM NAPDH, 50 $\mu g \cdot mL^{-1}$ GAPDH (enzyme fraction after heat precipitation), 1.45 $\mu g \cdot mL^{-1}$ purified PGK, 5 mM 3-PG and 0, 0.2, 0.4, 0.6, 1 or 2 mM ADP.

Half-life times of DHAP and GAP

Half-life times of DHAP and D,L-GAP were assayed under standard assay conditions. A reaction mixture of 0.1 M Tris/HCl (pH 6.5, 70 °C), 20 mM $MgCl_2$ (total volume of 760 μL) was pre-incubated for 3 min in a thermoblock to reach 70 °C. Subsequently, 5 mM final concentration DHAP and GAP was added and samples were withdrawn and stored on ice. The remaining GAP and DHAP were determined enzymatically in a continuous assay at 37 °C (340 nm). 100 μL of the reaction sample was transferred to 0.1 M Tris/HCl (pH 7.5, room temperature) containing 0.15 M sodium arsenate, 10 mM NAD^+, 5 mM $MgCl_2$, 10 U GAPDH (*Saccharomyces cerevisiae*, Sigma-Aldrich) and for DHAP detection an additional 8 U TPI (rabbit muscle; Sigma-Aldrich) in a total volume of 500 μL. The concentration decrease with time was fitted to an exponential decay curve and the half-life time was calculated from the fitted exponent.

Network reconstitution assay

Reconstitution assays with the four enzymes were performed in the following incubation buffer: 0.1 M Tris/HCl (pH 6.5, 70 °C), 20 mM $MgCl_2$, with 10 mM ATP, 0.2 mM NAPDH, 10 mM glucose, 5 mM PEP, 3 $\mu g \cdot mL^{-1}$ Sso-GDH (purified protein after gel filtration [38]), 40 $\mu g \cdot mL^{-1}$ Sso-PK (enriched fraction after heat precipitation at 80 °C). The following concentrations of enzymes were used for the standard incubation: 3.6 $\mu g \cdot mL^{-1}$ FBPA/ase, 0.85 $\mu g \cdot mL^{-1}$ TPI, 42.1 $\mu g \cdot mL^{-1}$ GAPDH, 3.4 $\mu g \cdot mL^{-1}$ PGK. The assay mixture was pre-incubated for 3 min to reach 70 °C and started by the addition of 3-PG (final concentration of 2 mM). Aliquots were withdrawn over a 200-min time period and the reaction was stopped by incubation on ice.

Determination of intermediate concentrations

The amounts of F6P, 3-PG, DHAP, GAP, PYR and BPG were quantified at 25 °C using mesophilic auxiliary enzymes in 500 μL total volume in Tris/HCl (pH 7, room temperature) buffer. (a) F6P was quantified out of 50 μL samples comprising 2 mM $NADP^+$, 1 U glucose 6-phosphate dehydrogenase (*S. cerevisiae*, Sigma-Aldrich) and 3 U phosphoglucoisomerase (*S. cerevisiae*, Sigma-Aldrich). (b) For the determination of DHAP concentration aliquots (70 μL) of the reactants were incubated in the presence of 0.1 mM NADH and α-glycerophosphate dehydrogenase (rabbit muscle, Sigma-Aldrich). After completion of the reaction 1 U TPI (rabbit muscle, Sigma-Aldrich) was added to determine the GAP concentration. (c) Detection of residual 3-PG concentrations were performed by incubation of a 5 μL reaction sample with 0.1 mM NADH, 2 mM ATP, 20 mM $MgCl_2$, 10 U GAPDH (*S. cerevisiae*, Sigma-Aldrich) and 6 U 3-phosphoglyceric phosphokinase (*S. cerevisiae*, Sigma-Aldrich). (d) Concentrations of BPG (samples of 100 μL) were determined in an assay containing 0.1 mM NADH and 10 U GAPDH (*S. cerevisiae*, Sigma-Aldrich). (e) The PK-dependent formation of pyruvate was detected in 10 μL aliquots in the presence of lactate dehydrogenase (Sigma-Aldrich) and 0.1 mM NADH in Tris/HCl buffer (pH 7, room temperature).

Computational methods

All computational analyses were performed in MATHEMATICA [41]. The NMinimize function was used for the fitting of kinetic rate equations to the experimental data sets for the isolated enzymes. An objective function based on the sum of the squared differences between the measured data and the enzyme kinetic rate equation was minimized with respect to all the parameter values in the equation. Solutions for the minimization were constrained to positive values for the parameters.

To analyse the sensitivity of the model predictions for small changes in parameter values, a large number of simulations (10 000) were run with randomly sampled parameters from a range 5% ± the measured value. Extreme values from the simulation results were taken for each of the intermediates at minute time point intervals. Further increasing the number of simulations did not significantly increase the extreme values.

Two mathematical models are used in the paper, a three-variable model (for steady state analysis) and a nine-variable model to simulate the conversion of 3-PG to F6P. The complete model descriptions are available as SBML files and can be simulated on the JWS Online website (http://jjj.mib.ac.uk).

Acknowledgements

The authors thank P. Schönheit (Christian-Albrechts-Universiteit Kiel, Germany) for providing the expression vector for the G6PDH of *T. maritima*, R. Hensel (Universiteit Duisburg-Essen, Germany) for providing the expression vectors of the *T. tenax* enzymes and

M. Zaparty (University of Regensburg, Germany) for cloning of the *fbpA/ase* gene. We acknowledge the financial assistance of the BBSRC (JLS and HVW via SysMO grants) and BMBF (TK and BS via SysMO grant SulfoSys, P-N-01-09-23, and SulfoSYSBIOTECH, 0316188A). JLS is supported by the South African Research Chairs Initiative of the Department of Science and Technology and National Research Foundation of South Africa.

References

1 Stetter KO (1999) Extremophiles and their adaptation to hot environments. *FEBS Lett* **452**, 22–25.
2 Daniel RM & Cowan DA (2000) Biomolecular stability and life at high temperatures. *Cell Mol Life Sci* **57**, 250–264.
3 Kawashima T, Amano N, Koike H, Makino SI, Higuchi S, Kawashima-Ohya Y, Watanabe K, Yamazaki M, Kanehori K, Kawamoto T *et al.* (2000) Archaeal adaptation to higher temperatures revealed by genomic sequence of *Thermoplasma volcanium*. *Proc Natl Acad Sci USA* **97**, 14257–14262.
4 Kouril T, Kolodkin A, Zaparty M, Steuer R, Ruoff P, Westerhoff HV, Snoep JL, Siebers B & consortium, SulfoSYS (2012) Sulfolobus Systems Biology: Cool Hot Design for Metabolic Pathways. Horizon Scientific Press and Caister Academic Press, Norwich.
5 Imanaka T & Atomi H (2002) Catalyzing 'hot' reactions: enzymes from hyperthermophilic archaea. *Chem Rec* **2**, 149–163.
6 Schramm A, Kohlhoff M & Hensel R (2001) Triose-phosphate isomerase from *Pyrococcus woesei* and *Methanothermus fervidus*. *Meth Enzymol* **331**, 62–77.
7 Ahmed H, Ettema TJG, Tjaden B, Geerling ACM, Van Der Oost J & Siebers B (2005) The semi-phosphorylative Entner–Doudoroff pathway in hyperthermophilic archaea: a re-evaluation. *Biochem J* **390**, 529–540.
8 Brunner NA, Brinkmann H, Siebers B & Hensel R (1998) NAD^+-dependent glyceraldehyde-3-phosphate dehydrogenase from *Thermoproteus tenax*. *J Biol Chem* **273**, 6149–6156.
9 Brunner NA, Siebers B & Hensel R (2001) Role of two different glyceraldehyde-3-phosphate dehydrogenases in controlling the reversible Embden–Meyerhof–Parnas pathway in *Thermoproteus tenax*: regulation on protein and transcript level. *Extremophiles* **5**, 101–109.
10 Lorentzen E, Hensel R, Knura T, Ahmed H & Pohl E (2004) Structural basis of allosteric regulation and substrate specificity of the non-phosphorylating glyceraldehyde 3-phosphate dehydrogenase from *Thermoproteus tenax*. *J Mol Biol* **341**, 815–828.
11 Ettema TJG, Ahmed H, Geerling ACM, Van Der Oost J & Siebers B (2008) The non-phosphorylating glyceraldehyde-3-phosphate dehydrogenase (gapn) of *Sulfolobus solfataricus*: a key-enzyme of the semi-phosphorylative branch of the Entner–Doudoroff pathway. *Extremophiles* **12**, 75–88.
12 Zaparty M, Zaigler A, Stamme C, Soppa J, Hensel R & Siebers B (2008) DNA microarray analysis of the central carbohydrate metabolism: glycolytic/gluconeogenic carbon switch in the hyperthermophilic crenarchaeum *Thermoproteus tenax*. *J Bacteriol* **190**, 2231–2238.
13 Say RF & Fuchs G (2010) Fructose 1,6-bisphosphate aldolase/phosphatase may be an ancestral gluconeogenic enzyme. *Nature* **464**, 1077–1081.
14 Matsubara K, Yokooji Y, Atomi H & Imanaka T (2011) Biochemical and genetic characterization of the three metabolic routes in *Thermococcus kodakarensis* linking glyceraldehyde 3-phosphate and 3-phosphoglycerate. *Mol Microbiol* **81**, 1300–1312.
15 Zillig W, Stetter KO & Wunderl S (1980) The Sulfolobus-'Caldariella' group: taxonomy on the basis of the structure of DNA-dependent RNA polymerases. *Arch Microbiol* **125**, 259–269.
16 Albers SV, Birkeland NK, Driessen AJM, Gertig S, Haferkamp P, Klenk HP, Kouril T, Manica A, Pham TK, Ruoff P *et al.* (2009) Sulfosys (sulfolobus systems biology): towards a silicon cell model for the central carbohydrate metabolism of the archaeon *Sulfolobus solfataricus* under temperature variation. *Biochem Soc Trans* **37**, 58–64.
17 Lamble HJ, Heyer NI, Bull SD, Hough DW & Danson MJ (2003) Metabolic pathway promiscuity in the archaeon *Sulfolobus solfataricus* revealed by studies on glucose dehydrogenase and 2-keto-3-deoxygluconate aldolase. *J Biol Chem* **278**, 34066–34072.
18 Lamble HJ, Theodossis A, Milburn CC, Taylor GL, Bull SD, Hough DW & Danson MJ (2005) Promiscuity in the part-phosphorylative Entner–Doudoroff pathway of the archaeon *Sulfolobus solfataricus*. *FEBS Lett* **579**, 6865–6869.
19 Snijders APL, Walther J, Peter S, Kinnman I, De Vos MGJ, Van De Werken HJG, Brouns SJJ, Van Der Oost J & Wright PC (2006) Reconstruction of central carbon metabolism in *Sulfolobus solfataricus* using a two-dimensional gel electrophoresis map, stable isotope labelling and DNA microarray analysis. *Proteomics* **6**, 1518–1529.
20 Van Der Oost J & Siebers B (2007) The Glycolytic Pathways of Archaea: Evolution by Tinkering. Vol. **1**, pp. 247–259. Blackwell Publishing, Singapore.
21 Zaparty M & Siebers B (2011) Reconstruction of the central carbon metabolic network of thermoacidophilic Archaea. In *Physiology, Metabolism and Enzymology of*

Thermoacidophiles (Horikoshi K, ed). Vol. **1**, pp. 602–639. Springer, Tokyo.
22 Potters MB, Solow BT, Bischoff KM, Graham DE, Lower BH, Helm R & Kennelly PJ (2003) Phosphoprotein with phosphoglycerate mutase activity from the archaeon *Sulfolobus solfataricus*. *J Bacteriol* **185**, 2112–2121.
23 Dello Russo A, Rullo R, Masullo M, Ianniciello G, Arcari P & Bocchini V (1995) Glyceraldehyde-3-phosphate dehydrogenase in the hyperthermophilic archaeon *Sulfolobus solfataricus*: characterization and significance in glucose metabolism. *Biochem Mol Biol Int* **36**, 123–135.
24 Hess D, Kruger K, Knappik A, Palm P & Hensel R (1995) Dimeric 3-phosphoglycerate kinases from hyperthermophilic archaea. Cloning, sequencing and expression of the 3-phosphoglycerate kinase gene of *Pyrococcus woesei* in *Escherichia coli* and characterization of the protein. Structural and functional comparison with the 3-phosphoglycerate kinase of *Methanothermus fervidus*. *Eur J Biochem* **233**, 227–237.
25 Jones CE, Fleming TM, Cowan DA, Littlechild JA & Piper PW (1995) The phosphoglycerate kinase and glyceraldehyde-3-phosphate dehydrogenase genes from the thermophilic archaeon *Sulfolobus solfataricus* overlap by 8 bp – isolation, sequencing of the genes and expression in *Escherichia coli*. *Eur J Biochem* **233**, 800–808.
26 Du J, Say RF, Lu W, Fuchs G & Einsle O (2011) Active-site remodelling in the bifunctional fructose-1,6-bisphosphate aldolase/phosphatase. *Nature* **478**, 534–537.
27 Fushinobu S, Nishimasu H, Hattori D, Song HJ & Wakagi T (2011) Structural basis for the bifunctionality of fructose-1,6-bisphosphate aldolase/phosphatase. *Nature* **478**, 538–541.
28 König H, Skorko R, Zillig W & Reiter WD (1982) Glycogen in thermoacidophilic archaebacteria of the genera Sulfolobus, Thermoproteus, Desulfurococcus and Thermococcus. *Arch Microbiol* **132**, 297–303.
29 Maruta K, Mitsuzumi H, Nakada T, Kubota M, Chaen H, Fukuda S, Sugimoto T & Kurimoto M (1996) Cloning and sequencing of a cluster of genes encoding novel enzymes of trehalose biosynthesis from thermophilic archaebacterium *Sulfolobus acidocaldarius*. *Biochim Biophys Acta (BBA) General Subjects* **1291**, 177–181.
30 Park HS, Park JT, Kang HK, Cha H, Kim DS, Kim JW & Park KH (2007) TreX from *Sulfolobus solfataricus* ATCC 35092 displays isoamylase and 4-α-glucanotransferase activities. *Biosci Biotechnol Biochem* **71**, 1348–1352.
31 Woo EJ, Lee S, Cha H, Park JT, Yoon SM, Song HN & Park KH (2008) Structural insight into the bifunctional mechanism of the glycogen-debranching enzyme TreX from the archaeon *Sulfolobus solfataricus*. *J Biol Chem* **283**, 28641–28648.
32 Hofmeyr JH & Cornish-Bowden A (1997) The reversible Hill equation: how to incorporate cooperative enzymes into metabolic models. *Cabios* **13**, 377–385.
33 Hanekom AJ (2006) Generic rate equations for modelling multisubstrate reactions in computational systems biology. Master's thesis, Stellenbosch University, South Africa.
34 Ito F, Chishiki H, Fushinobu S & Wakagi T (2012) Comparative analysis of two glyceraldehyde-3-phosphate dehydrogenases from a thermoacidophilic archaeon, *Sulfolobus tokodaii*. *FEBS Lett* **586**, 3097–3103.
35 Siebers B, Tjaden B, Michalke K, Dörr C, Ahmed H, Zaparty M, Gordon P, Sensen CW, Zibat A & Klenk HP, *et al.* (2004) Reconstruction of the central carbohydrate metabolism of *Thermoproteus tenax* by use of genomic and biochemical data. *J Bacteriol* **186**, 2179–2194.
36 Dörr C, Zaparty M, Tjaden B, Brinkmann H & Siebers B (2003) The hexokinase of the hyperthermophile *Thermoproteus tenax:* ATP-dependent hexokinases and ADP-dependent glucokinases, two alternatives for glucose phosphorylation in archaea. *J Biol Chem* **278**, 18744–18753.
37 Hansen T, Schlichting B & Schönheit P (2002) Glucose-6-phosphate dehydrogenase from the hyperthermophilic bacterium *Thermotoga maritima*: expression of the g6pd gene and characterization of an extremely thermophilic enzyme. *FEMS Microbiol Lett* **216**, 249–253.
38 Haferkamp P, Kutschki S, Treichel J, Hemeda H, Sewczyk K, Hoffmann D, Zaparty M & Siebers B (2011) An additional glucose dehydrogenase from *Sulfolobus solfataricus*: fine-tuning of sugar degradation? *Biochem Soc Trans* **39**, 77–81.
39 Haferkamp P (2011) *Biochemical studies of enzymes involved in glycolysis of the thermoacidophilic crenarchaeon* Sulfolobus solfataricus. PhD thesis, University of Duisburg-Essen, Germany.
40 Littlechild JA & Isupov M (2001) Glyceraldehyde-3-phosphate dehydrogenase from *Sulfolobus solfataricus*. In Methods in Enzymology, Vol. 331: Hyperthermophilic Enzymes, Part B (Michael WW & Adams RMK, eds), pp. 105–117. Academic Press, San Diego, CA.
41 Wolfram Research Inc. (2010) Mathematica Edition: Version 8.0. Wolfram Research Inc., Champaign, IL.

Supporting information

Additional supporting information may be found in the online version of this article at the publisher's web site:

Doc. S1. Sensitivity analysis for the minimal steady state model.